Electronic Supplementary Material (ESI) for New Journal of Chemistry.

Hydrogen bonded networks based on hexarhenium(III) chalcocyanide clusters complexes: structural and photophysical characterizations

Alexandra Ledneva,[a] Sylvie Ferlay,[b*] Nikolay G. Naumov,[a,c] Matteo Mauro,[b] Stéphane Cordier,[d] Nathalie Kyritsakas,[b] Mir Wais Hosseini[b*]

	(**1**-2H)$_2$-[Re$_6$S$^i_8$(CN)$^a_6$]	(**1**-2H)$_2$-[Re$_6$Se$^i_8$(CN)$^a_6$]	(**2**-2H)$_2$-[Re$_6$S$^i_8$(CN)$^a_6$]	(**2**-2H)$_2$-[Re$_6$Se$^i_8$(CN)$^a_6$]
C-N (cation)	1.304(4) 1.308(4) 1.310(4) 1.313(4)	1.306(4) 1.310(4) 1.312(4)	1.310(6) 1.313(6)	1.283(14) 1.346(15)
C ≡N	1.146(4) 1.152(4) 1.161(4)	1.146(5) 1.150(4) 1.143(4)	1.145(6) 1.157(7) 1.146(6)	1.146(14) 1.160(13) 1.173(14)
Re-C	2.111(3) 2.102(3) 2.116(3)	2.107(4) 2.111(3) 2.115(3)	2.115(5) 2.118(5) 2.123(5)	2.113(11) 2.102(10) 2.106(12)
Re-Q (Q = S or Se)	2.4007(7) 2.4024(7) 2.4032(8) 2.4038(7) 2.4040(7) 2.4045(7) 2.4052(7) 2.4053(7) 2.4062(7) 2.4075(8) 2.4077(8) 2.4123(7) 2.4128(7)	2.5130(3) 2.5139(3) 2.5145(3) 2.5146(3) 2.5150(3) 2.5177(3) 2.5184(3) 2.5188(3) 2.5220(3) 2.5248(3) 2.5249(3) 2.5271(3) 2.5272(3) 2.5273(3)	2.3957(12) 2.3960(12) 2.4007(12) 2.4079(12) 2.4010(12) 2.4035(11) 2.4080(11) 2.4129(12) 2.4016(13) 2.4022(13) 2.4036(12) 2.4043(12) 2.4036(12) 2.4129(12) 2.4007(12	2.5164(9) 2.5173(12) 2.5278(12) 2.5284(10) 2.5132(12) 2.5178(12) 2.5204(11) 2.5220(11) 2.5066(10) 2.5167(10) 2.5233(12) 2.5355(12) 2.5219(11) 2.5284(10)
Re-Re	2.59751(16) 2.59972(16) 2.59973(16) 2.59989(17) 2.60543(17)	2.62498(19) 2.62502(17) 2.62930(17) 2.62963(17) 2.62965(17) 2.63011(17) 2.63012(17) 2.63076(17) 2.63671(19)	2.5903(3) 2.6011(3) 2.6015(3) 2.6051(3) 2.5987(3) 2.6060(3)	2.6218(6) 2.6248(6) 2.6389(6) 2.6439(5) 2.6219(6) 2.6316(6) 2.6317(5)
N-H-N	2.849(4) 2.932(4) 3.008(5) 3.107(5)	2.844(4) 2.946(4) 3.085(4) 3.017(4)	2.875(7) 3.017(8) 3.021(9) 3.098(8)	2.904(12) 3.003(15) 3.020(17) 3.036(16)

Table S1: Useful bonds and distances for (**1**-2H)$_2$-[Re$_6$Q$^i_8$(CN)$^a_6$] (Q=S or Se) and (**2**-2H)$_2$-[Re$_6$Q$^i_8$(CN)$^a_6$] (Q=S or Se).

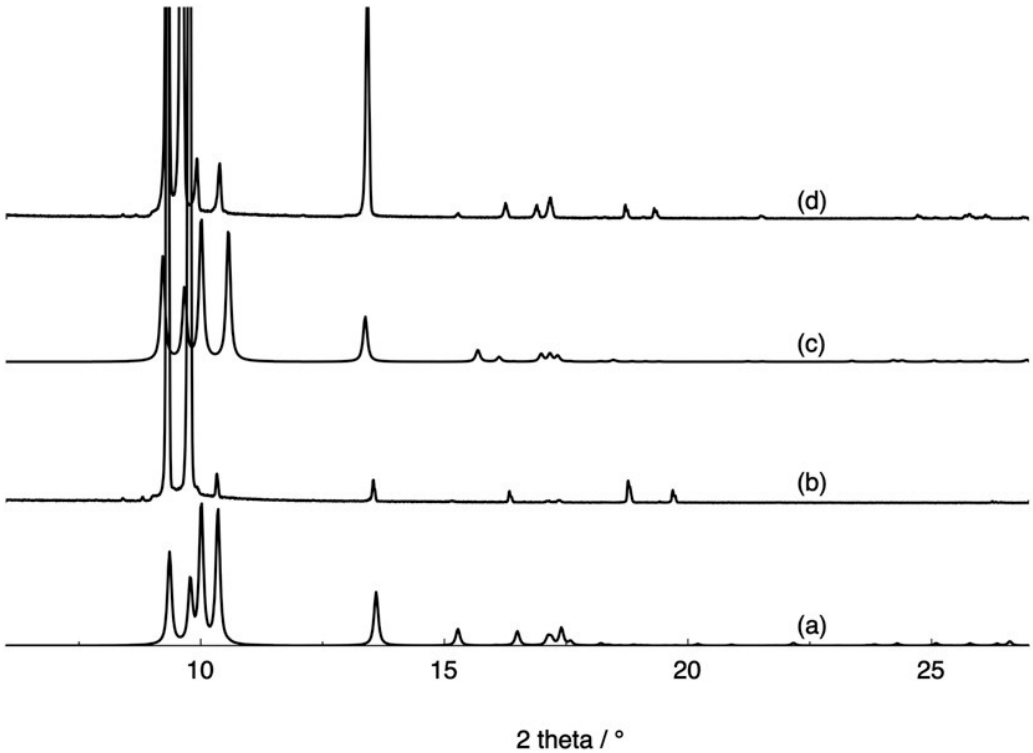

Figure S1: Comparison of the simulated (a) (**1**-2H)$_2$-[$Re_6S^i_8(CN)^a_6$] and (c) (**1**-2H)$_2$-[$Re_6Se^i_8(CN)^a_6$], and recorded PXRD patterns for (**1**-2H)$_2$-[$Re_6S^i_8(CN)^a_6$] (b) (**1**-2H)$_2$-[$Re_6Se^i_8(CN)^a_6$], (d). Discrepancies in intensity between the observed and simulated patterns are due to preferential orientations of the microcrystalline powders.

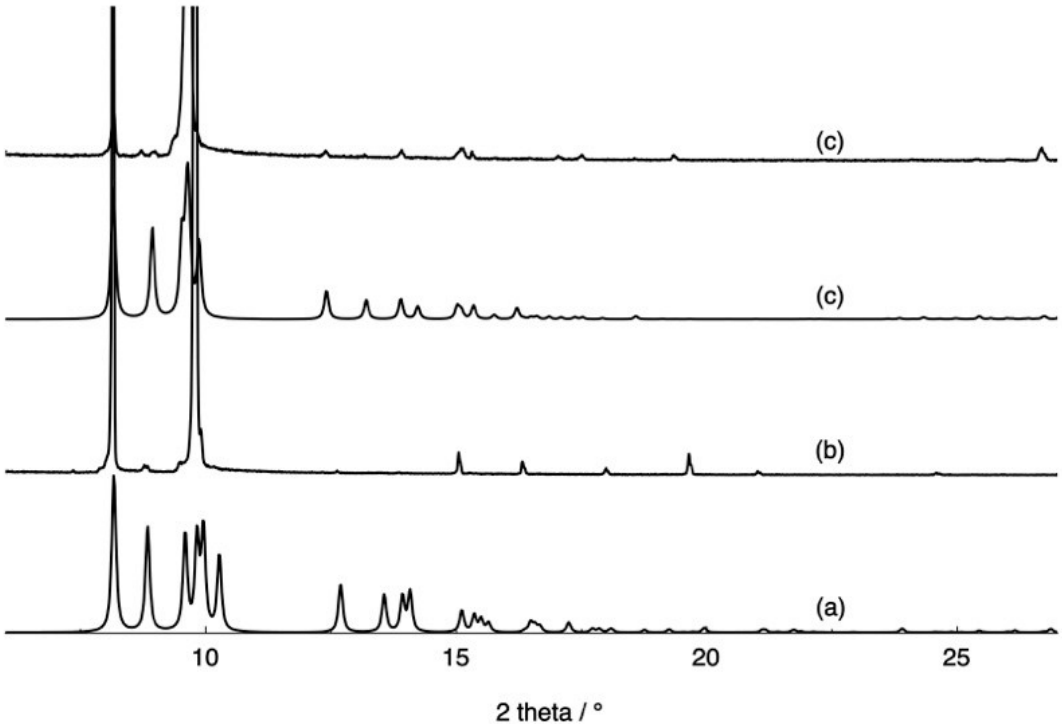

Figure S2: Comparison of the simulated (a) (**2**-2H)$_2$-[$Re_6S^i_8(CN)^a_6$] and (c) (**2**-2H)$_2$-[$Re_6Se^i_8(CN)^a_6$] and recorded PXRD patterns for (**2**-2H)$_2$-[$Re_6S^i_8(CN)^a_6$] (b) and (**2**-2H)$_2$-[$Re_6Se^i_8(CN)^a_6$] (d). Discrepancies in intensity between the observed and simulated patterns are due to preferential orientations of the microcrystalline powders.